Flavopiridol Induces Apoptosis in Glioma Cell Lines Independent of Retinoblastoma and p53 Tumor Suppressor Pathway Alterations by a Caspase-independent Pathway[1]

Michelle Alonso, Cristina Tamasdan, Douglas C. Miller, and Elizabeth W. Newcomb[2]

Department of Pathology [M. A., C. T., D. C. M., E. W. N.] and Division of Neuropathology [D. C. M.], and New York University Cancer Institute and Kaplan Comprehensive Cancer Center [D. C. M., E. W. N.], New York University School of Medicine, New York, New York 10016

Abstract

Flavopiridol is a synthetic flavone, which inhibits growth *in vitro* and *in vivo* of several solid malignancies such as renal, prostate, and colon cancers. It is a potent cyclin-dependent kinase inhibitor presently in clinical trials. In this study, we examined the effect of flavopiridol on a panel of glioma cell lines having different genetic profiles: five of six have codeletion of $p16^{INK4a}$ and $p14^{ARF}$; three of six have *p53* mutations; and one of six shows overexpression of mouse double minute-2 (MDM2) protein. Independent of retinoblastoma and p53 tumor suppressor pathway alterations, flavopiridol induced apoptosis in all cell lines but through a caspase-independent mechanism. No cleavage products for caspase 3 or its substrate poly(ADP-ribose) polymerase or caspase 8 were detected. The pan-caspase inhibitor Z-VAD-fmk did not inhibit flavopiridol-induced apoptosis. Mitochondrial damage measured by cytochrome *c* release and transmission electron microscopy was not observed in drug-treated glioma cells. In contrast, flavopiridol treatment induced translocation of apoptosis-inducing factor from the mitochondria to the nucleus. The proteins cyclin D_1 and MDM2 involved in the regulation of retinoblastoma and p53 activity, respectively, were down-regulated early after flavopiridol treatment. Given that MDM2 protein can confer oncogenic properties under certain circumstances, loss of MDM2 expression in tumor cells could promote increased chemosensitivity. After drug treatment, a low Bcl-2/Bax ratio was observed, a condition that may favor apoptosis. Taken together, the data indicate that flavopiridol has activity against glioma cell lines *in vitro* and should be considered for clinical development in the treatment of glioblastoma multiforme.

Introduction

GBM[3] are largely refractory to radiation and other adjuvant therapies in use today, in part, accounting for the poor survivals of affected patients, generally much less than 24 months. Resistance to treatment may be associated with deregulation of the two major cell cycle pathways: Rb ($p16^{INK4a}$, cyclin D_1, CDK4) and p53 ($p14^{ARF}$, MDM2, $p21^{WAF1}$) tumor suppressor pathways. Alterations of these pathways occur in the majority of human cancers, implicating these two genetic pathways in tumor development (1). Disruption of the Rb cell cycle control pathway occurs in 80% of adult GBM through loss of $p16^{INK4a}$ function via gene deletion, amplification of CDK4, or mutation in Rb (2, 3). The p53 protein plays a central role in the signaling pathways required to mediate apoptosis (4). It interacts with the promoters of many different genes and can directly up-regulate $p21^{WAF1}$, MDM2, and Bax expression (5). Mutations inactivate the *p53* gene in >50% of GBM, and overexpression of MDM2 occurs in ~50% of the cases (6, 7). MDM2 both inhibits the transcriptional activity of p53 and can target p53 for degradation. In glioma cell lines, overexpression of MDM2 has been associated with drug resistance (8, 9). Consequently, deregulation of the Rb and/or p53 growth control pathways in GBM may interfere with chemotherapy-induced apoptosis (10, 11).

Flavopiridol [5,7-dihydroxy-8-(4-N-methyl-2-hydroxypyridyl)-6′-chloroflavone hydrochloride, L86–8275, HMR 1275] is a synthetic flavone closely related to a compound found in a plant native to India, *Dysoxylum binectariferum* (12). Currently, the drug is in Phase I and II clinical trials as an antineoplastic agent for breast, gastric, and renal cancers (13–17). The drug is a potent inhibitor of most CDKs, including CDK1, CDK2, CDK4, and CDK7 (18). It induces growth arrest at either the G_1 and/or G_2 phases of the cell cycle in numerous cell lines *in vitro* by acting as a competitive binding agent for the ATP-binding pocket of CDK (18). One consequence of this inhibition is a decrease in cyclin D_1, the

Received 8/30/02; revised 12/2/02; accepted 12/20/02.
The costs of publication of this article were defrayed in part by the payment of page charges. This article must therefore be hereby marked *advertisement* in accordance with 18 U.S.C. Section 1734 solely to indicate this fact.
[1] Supported by NIH Grant CA90290 and grants from the National Brain Tumor Foundation, Children's Brain Tumor Foundation, and Elsa U. Pardee Foundation (to E. W. N.).
[2] To whom requests for reprints should be addressed, at Department of Pathology, New York University School of Medicine and Kaplan Comprehensive Cancer Center, 550 First Avenue, New York, NY 10016. Phone: (212) 263-8757; Fax: (212) 263-8211; E-mail: newcoe01@med.nyu.edu.

[3] The abbreviations used are: GBM, glioblastoma multiforme; MDM2, mouse double minute-2; CDK, cyclin-dependent kinase; Rb, retinoblastoma; PARP, poly(ADP-ribose) polymerase; PI, propidium iodide; DAPI, 4′,6-diamidino-2-phenylindole; Z-VAD-fmk, N-benzyloxycarbonyl-Val-Ala-Asp-fluoromethylketone; AIF, apoptosis-inducing factor.

binding partner of CDK4 in G_1, by depletion of cyclin D_1 mRNA resulting in a decrease in CDK4 kinase activity (19).

In this study, we wished to examine the effect of flavopiridol on a panel of glioma cell lines, which have alterations in both the Rb and p53 tumor suppressor pathways. Five of six cell lines have deletions of the CDK inhibitor $p16^{INK4a}$ (all except CCF-STTG1) inactivating the Rb cell cycle control pathway. The cell lines express either wild-type p53 (A172, CCF-STTG1, and U87MG) or mutant p53 (T98G, U118MG, and U251MG), whereas one of six cell lines overexpresses MDM2 protein (CCF-STTG1), which acts to disrupt the p53 cell cycle pathway (Fig. 1; Refs. 20–22). We found two novel findings in glioma cell lines treated with flavopiridol. First, flavopiridol induces apoptosis through a caspase-independent mechanism in all of the glioma cell lines. Second, flavopiridol decreased expression of both MDM2 mRNA and protein by 24 h in all of the cell lines independent of Rb or p53 tumor suppressor pathway alterations. Taken together, the data indicates that flavopiridol has activity against glioma cell lines *in vitro* and should be considered for clinical development in the treatment of GBM.

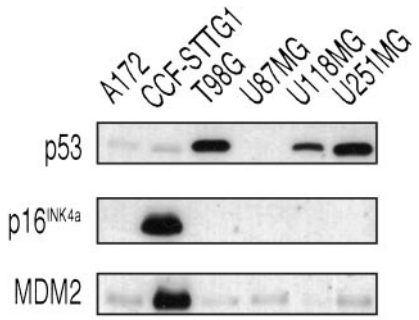

Fig. 1. Western blot analysis of gene expression in glioma cell lines. The cell lines A172, CCF-STTG1, and U87MG express wild-type p53, whereas T98G, U118MG, and U251MG express mutant p53. All of the cell lines in the panel have deletions of the CDK inhibitor $p16^{INK4a}$, except CCF-STTG1. Although all of the cell lines express MDM2, only CCF-STTG1 showed up-regulation of MDM2 protein expression because of amplification of the MDM2 gene.

Materials and Methods

Cell Culture. Glioma cell lines (A172, CCF-STTG1, T98G, U87MG, U118MG, U251MG, and U373MG) were obtained from the American Type Culture Collection (Manassas, VA). The HL-60 promyelocytic leukemia cell line was also obtained from the American Type Culture Collection. Cell lines were cultured in 5% CO_2 and 95% humidified air atmosphere at 37°C in DMEM (Life Technologies, Inc., Grand Island, NY), except for CCF-STTG1 and HL-60, which were maintained in RPMI 1640 (Mediatech Cellgro, Pittsburgh, PA). Media was supplemented with 10% (all glioma cell lines) or 20% (HL-60 cells) fetal bovine serum (Atlanta Biologicals, Norcross, GA), 100 units/liter penicillin, 100 μg/ml streptomycin, and 2 mM glutamine (Life Technologies, Inc.). Cells were split every 3 days to ensure logarithmic growth. For cytotoxicity studies, flavopiridol (Aventis Pharmaceuticals, Bridgewater, NJ) was dissolved in water, and stock solution (4 mg/ml) was stored at −20°C.

Assessment of Cell Viability. To assess cell viability, triplicate samples were removed from each culture condition at the appropriate time interval, diluted 1:10 with trypan blue, and counted. The percentage of cells scoring positive for uptake of the dye was calculated using the following formula: (number of trypan blue positive cells/number of trypan blue-positive cells + number of trypan blue negative cells) × 100.

Time Course of Drug-induced Apoptosis and Inhibitor Studies. For the time course experiments, glioma cells (4.5×10^5) were plated in 10-cm dishes (Nalge Nunc International, Naperville, IL) in 10 ml of medium for 14–16 h at 37°C before the addition of 300 nM flavopiridol. Adherent and nonadherent cells (total cells) were harvested at the appropriate time interval, washed with ice-cold PBS, and subjected to lysis and protein extraction. The HL-60 cells (2×10^6) were grown in suspension cultures in 3 ml of medium for 24 h at 37°C before the addition of 200 nM flavopiridol. Total cells were collected at the appropriate time interval and processed for Western blot analysis.

For the inhibitor studies, cells were either treated with an equivalent volume of inhibitor vehicle (DMSO ≤ 0.1%) or were pretreated with 100 μM Z-VAD-fmk (Enzyme Systems Products, Livermore, CA) for 2 h at 37°C. Cells were then left untreated or treated with 300 nM flavopiridol. Cells were collected after drug treatment at the appropriate time interval, washed with ice-cold PBS, and lysed for protein extraction with subsequent Western blotting.

Flow Cytometric Analysis. For cell cycle analysis, total cells were harvested from each culture condition at the appropriate time interval, washed in ice-cold PBS, resuspended in 400 μl of ice-cold PBS, and diluted by dropwise addition of 1 ml of 100% ethanol. After fixation of ≥1 h at 4°C, cells were washed with ice-cold PBS and resuspended in 300 μl of a RNase A/PI mixture containing 0.5 mg/ml RNase A and 50 μg/ml PI in PBS and incubated at room temperature for a minimum of 1 h. DNA content was used to distinguish each cell cycle phase using flow cytometry. To monitor changes in cell membrane integrity during drug treatment, the annexin V apoptosis detection kit (Biovision, Moutain View, CA) that characterizes phosphatidylserine exposure associated with an early loss of cell membrane integrity was used following the manufacturer's recommendations. Briefly, cells (1×10^5 in 100 μl) were washed twice in ice-cold PBS and resuspended in binding buffer. After adding annexin V with FITC and PI, the cells were incubated in the dark at room temperature for 5 min. Binding buffer was added, and the samples were analyzed by flow cytometry. Flow cytometry was performed on a Becton Dickinson FACScan (San Jose, CA).

DNA Fragmentation Assay. Total cells (5×10^5) were harvested from each culture condition at the appropriate time interval and centrifuged at 2000 rpm at room temperature. Supernatants were removed, and the pelleted cells were resuspended in 20 μl of lysis buffer [20 mM EDTA, 100 mM Tris-HCl (pH 8.0), and 0.8% sodium lauronyl sarcosine; all from Sigma-Aldrich, St. Louis, MO]. After complete resuspension, 10 μl of a 1 mg/ml RNase/T1 mixture mix (Ambion, Austin, TX) was added, and the lysed cells were incubated in a 37°C water bath for 1.5 h. Upon completion of this incu-

bation, 10 μl of 20 mg/ml proteinase K (Roche Molecular Biochemicals, Mannheim, Germany) were added to each sample followed by incubation for at least 16 h at 50°C with constant rotation. The recovered DNA (10 μl/sample) was electrophoresed on 1.0% agarose gels containing 0.5% Gelstar nucleic acid stain (BioWhittaker Molecular Applications, Rockland, ME) in TAE buffer [40 nM Tris acetate (pH 8.0), and 2 mM EDTA] for 1.5 h at 55 V and visualized with a Bio-Rad Gel Doc apparatus (Bio-Rad, Hercules, CA) using Quantity One (version 4.2.1) software.

Immunohistochemistry for Cytochrome *c*, AIF, and DAPI. A172 cells (1×10^5) were either grown on cover slips placed in 35-mm dishes (Nalge Nunc International) in 3 ml of medium for 14–16 h at 37°C before the addition of the drug or harvested and plated (1×10^5) on a 12-well slide (63425-05; EM Science, Gibbstown, NJ) precoated with poly-D-lysine (0.1 mg/ml; Sigma-Aldrich) and allowed to adhere for 10 min at room temperature. Cells were washed twice with ice-cold PBS, fixed with 2% formaldehyde on ice for 30 min, washed three times in ice-cold PBS, and cells were permeabilized with 0.1% Triton-X in PBS on ice for 10 min. After washing the cultures three times with ice-cold PBS, cells were incubated either with mouse IgG (6011-0080, Cappel; ICN Biomedicals, Orangeburg, NY) in PBS (5 μg/ml), or rabbit serum (16120-099; Life Technologies, Inc.) in PBS (5%) was added to the cells at room temperature for 10 min to block nonspecific staining of the cells, respectively. For indirect immunohistochemistry, the mouse anticytochrome *c* monoclonal antibody at 1:100 (clone 6H2.B4; PharMingen, San Diego, CA) was used as the primary antibody overnight at 4°C, followed by the goat antimouse IgG-FITC at 1:100 (sc2010; Santa Cruz Biotechnology, Santa Cruz, CA) as the secondary for 30 min at room temperature. The rabbit anti-AIF polyclonal antibody at 1:500 (sc5586; Santa Cruz Biotechnology) was used as the primary antibody at room temperature for 4 h, followed by the goat antirabbit IgG-TRITC at 1:200 (no. 4010-03; Southern Biotechnology Associates, Inc., Birmingham, AL) as the secondary for 30 min at room temperature. Cells were counterstained with the DNA specific dye DAPI (Sigma-Aldrich) using 1:1000 of a 1 mg/ml stock for 15 min at room temperature. Cultures were washed three times with ice-cold PBS and mounted in mounting medium for fluorescence (H-1000; Vector Laboratories, Burlingame, CA) and viewed on a Nikon Eclipse inverted fluorescence microscope. Images were captured with a Real Time Slide camera (Diagnostic Instruments, St. Sterling Heights, MI) and visualized using Spot (version 3.4.3) software.

Transmission Electron Microscopy. A representative glioma cell line was selected for transmission electron microscopy studies. The A172 cell line was plated as described for the time course experiments. At 72 h, adherent and nonadherent cells were harvested from the control or drug-treated cultures and collected by centrifugation at 1200 rpm for 12 min. The cells were assessed for viability using the trypan blue assay. The untreated cultures contained 2% trypan blue positive cells, compared with >80% in the 72 h flavopiridol treated culture. Cells were placed in 1.5-ml Eppendorf tubes and pelleted for 4 min at 1300 rpm. Pellets were fixed in 2% glutaraldehyde at room temperature overnight and processed in a standard manner and embedded in Epon. Semithin plastic sections were cut at 1 μm and stained with Toluidine Blue to evaluate the quality of preservation. Ultrathin sections (70 nm) were cut, mounted on copper grids, and stained with Uranyl acetate by standard methods. Stained grids were examined and photographed in a Zeiss EM10 electron microscope.

Extraction of Proteins, Immunoblot, and Densitometric Analysis. Total cells were harvested from each culture condition at the appropriate time interval, washed with ice-cold PBS, and lysed in a buffer containing Triton X-100 and NP40 supplemented with protease inhibitors as described previously (23). Quantitation of protein was carried out with the BCA reagent (Pierce, Rockford, IL). Equal amounts of protein (30 μg) in the presence of 5% β-mercaptoethanol (Sigma-Aldrich) were electrophoresed on 7.5% (p53, MDM2, and PARP) or 12% ($p27^{Kip1}$, cyclin D_1, Bcl-2, Bax, caspase 3, and caspase 8) SDS-PAGE gels. The gels were subsequently transferred to Immobilon-P membranes (Millipore, Bedford, MA) by electroblotting at 4°C for 2 h at 90–100 V. Immunoblotting was performed as previously described (23) with the following antibodies: mouse antiactin monoclonal antibody used at 1:32,000 (clone C4; Chemicon International, Inc., Temecula, CA); rabbit anti-Bax polyclonal antibody used at 1:1000 (13666E; PharMingen, San Diego, CA); mouse anti-Bcl-2 monoclonal antibody used at 1:100 (clone 124; Dako, Glostrup, Denmark); mouse anti-caspase 3 polyclonal antibody used at 1:500 (556425; PharMingen); mouse anti-cyclin D_1 monoclonal antibody used at 1:500 (Ab-3, Oncogene Research Products, Boston, MA); mouse anti-MDM2 monoclonal antibody used at 2 μg/ml (OP46, Oncogene Research Products, Boston, MA); mouse anti-$p27^{Kip1}$ antibody used at 1:200 (clone 57, Transduction Laboratories, Lexington, KY); mouse anti-p53 monoclonal antibody used at 1:200 (Ab-2, Oncogene Research Products, Boston, MA); rabbit anti-caspase 8 polyclonal antibody used at 2.5 μg/ml (PC335, Oncogene Research Products, Boston, MA); and mouse anti-PARP monoclonal antibody used at 1:500 (clone C2–10; PharMingen). Monoclonal sheep antimouse IgG, donkey antirabbit IgG (both from Amersham Life Pharmacia Biotech, Piscataway, NJ), or antigoat IgG (Santa Cruz Biotechnology) horseradish peroxidase-conjugated secondary antibodies were used at 1:2000. Immunodetection was carried out with the Supersignal West Femto Maximum Sensitivity Substrate detection system (Pierce) followed by visualization and densitometry using the Bio-Rad Fluor-S apparatus (Bio-Rad) with Quantity One (version 4.2.1) software.

Cycloheximide Treatment. Cells (2×10^5) were cultured in 35-mm dishes (Nalge Nunc International) in 2 ml of medium for 14–16 h at 37°C followed by treatment with flavopiridol (300 nM) for 6 h before the addition of cycloheximide (100 μg/ml; Sigma-Aldrich). Total cells were harvested from each culture condition at the appropriate time interval, washed with ice-cold PBS, and subjected to lysis and protein extraction for Western blotting as described previously.

Northern Blot Analysis. Total cellular RNA was isolated from each cell culture condition using the RNeasy Mini Kit (Qiagen, Inc., Santa Clarita, CA). Total RNA (20 μg) was

resolved by formaldehyde gel electrophoresis, transferred to a nylon membrane (Amersham Life Pharmacia Biotech), and cross-linked by exposing the membrane to UV light for 5 min. Equivalent loading of RNA samples was confirmed by visualization of 18S and 28S rRNA. The MDM2, cyclin D_1, and p53 probes were kindly provided by Drs. Angel Pellicer and Michele Pagano (New York University School of Medicine, New York, NY). Probes were ^{32}P-labeled by using the Rediprime II labeling kit (Amersham Life Pharmacia Biotech). Membranes were hybridized with the probes overnight at 42°C in 50% formamide, 5× SSPE (4 M NaCl, 1 M sodium phosphate, and 0.5 M EDTA), 10% SDS, 5 mg/ml calf thymus DNA, and 100× Denhardt's solution and washed three times at 42°C with 2× SSC (150 mM NaCl and 15 mM sodium citrate) and 0.1% SDS. The radioactive signal on the membrane was visualized and quantitated using a Bio-Rad Personal FX Phosphoimager with Quantity One Software (version 4.2.1).

Results

Flavopiridol-induced Cytotoxicity and Decreased Cell Viability. Treatment of glioma cell lines for 72 h with 0–500 nM flavopiridol resulted in a dose-dependent inhibition of cell proliferation. All of the cell lines showed similar maximal drug-induced cytotoxicity at 72 h of treatment over the range of 200–500 nM concentrations of the drug (data not shown). Therefore, we chose the concentration of 300 nM for all additional experiments because it is the dose that reaches physiologically relevant median steady state plasma concentration of the drug detected in patients (13, 14).

Loss of membrane integrity of cells untreated or treated with 300 nM flavopiridol was determined by the uptake of the dye trypan blue over a 72-h interval. Representative data are shown for the A172 cell line expressing wild-type p53 and the T98G cell line expressing mutant p53 (Fig. 2). After treatment with flavopiridol, all six cell lines of the panel lost membrane integrity regardless of genetic alterations in the Rb and p53 tumor suppressor pathways as evidenced by cell viabilities decreasing from 70% at 48 h to <50% by 72 h.

Flavopiridol-induced Growth Arrest. Flow cytometry was used to determine DNA content and cell cycle phase. Table 1 summarizes cell cycle analysis of four glioma cell lines A172, U87MG, T98G, and U118MG. The glioma cell lines CCF-STTG1 and U251MG had similar cell cycle profiles as U87MG and U118MG, respectively (data not shown). All of the cell lines demonstrated growth arrest at G_2, as evidenced by a decrease in the proportion of cells in S phase and an increase in those in G_2 with no change in the proportion in G_1 (Table 1).

Flavopiridol-induced Apoptosis. Fluorescence-activated cell sorting analysis, DNA fragmentation, and annexin V/PI staining assays were used to monitor drug-induced apoptosis. Representative data are shown for the A172 cell line expressing wild-type p53 and the T98G cell line expressing mutant p53 (Table 1). The presence of the sub-G_1 peak in fluorescence-activated cell sorting cell cycle analysis (data not shown) indicates cell fragmentation generally interpreted as evidence of apoptosis (24). An increase in the sub-G_1 peak was evident in all of the cell lines by 72 h (Table 1). In addition, drug-induced apoptosis was demonstrated by DNA laddering (Fig. 3). By 48 h of flavopiridol treatment, fragmentation of DNA was apparent in A172 cells and by 72 h in T98G cells compared with the respective untreated control cultures. In addition, phosphatidylserine exposure was induced by flavopiridol treatment with the percentage of annexin V-positive cells showing a time-dependent increase over the 72-h interval from 8–37% (data not shown).

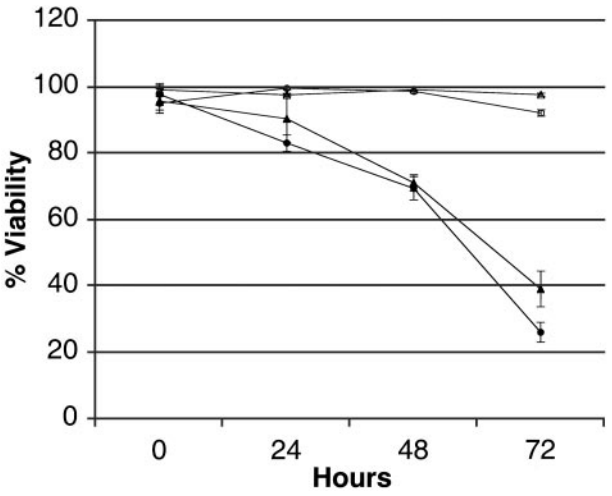

Fig. 2. Flavopiridol decreased cell viability. Loss of membrane integrity of cells untreated or treated with 300 nM flavopiridol was determined by the inability of cells to exclude the vital dye trypan blue. At the appropriate time interval, triplicate samples were removed from each culture and counted. The percentage of cells that remained viable was calculated from the total number of cells counted. Representative data are shown for the A172 cell line expressing wild-type p53 (*circles*), and the T98G cell line expressing mutant p53 (*triangles*). Untreated cells (*open symbols*) and flavopiridol treated cells (*closed symbols*), respectively. Maximal drug-induced cytotoxicity occurred at 72 h. The data presented are representative of three independent experiments.

Flavopiridol-induced Changes in the Expression of Cell Cycle Proteins. Changes in the expression of various cell cycle proteins were analyzed by Western blotting. Representative data are shown for the A172 cell line expressing wild-type p53 (Fig. 4*A*) and the T98G cell line expressing mutant p53 (Fig. 4*B*). Flavopiridol treatment of all six cell lines produced a complete loss of two proteins regardless of *p53* status. The expression of MDM2 decreased markedly after flavopiridol treatment for 12 h and was undetectable by 24 h. Similarly, the expression of cyclin D_1 decreased by 12 h and became undetectable by 24 or 48 h. p53 expression increased between 3 and 6 h in all cell lines expressing wild-type p53, whereas no increase occurred in any of the cell lines expressing mutant p53. In cell lines expressing wild-type p53, expression of $p27^{Kip1}$ decreased between 6 and 12 h and was absent by 48 h compared with cell lines expressing mutant p53 where $p27^{Kip1}$ protein expression was unchanged. For Bcl-2, protein expression decreased between 24 and 48 h after drug treatment and then remained at a decreased level in all of the cell lines. Bax protein levels increased in both the wild-type and mutant p53 cell lines by 24 and 48 h, respectively, after drug treatment. Cleavage of Bax from p21 to p18 was clearly evident at 48 h of drug

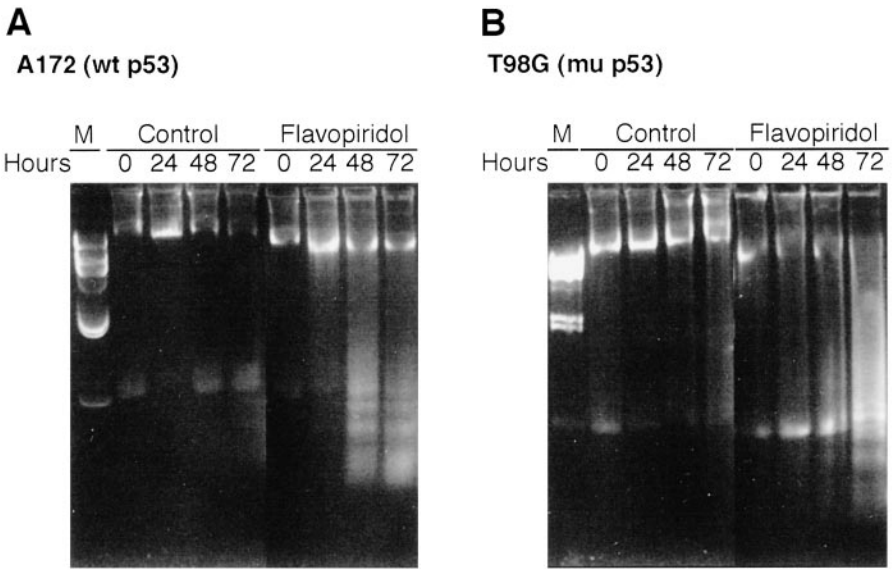

Fig. 3. Flavopiridol induced apoptosis. Representative data are shown for the A172 cell line expressing wild-type (*wt*) p53 (*A*) and the T98G cell line expressing mutant (*mu*) p53 (*B*). Cells were either left untreated or treated with 300 nM flavopiridol. Total cells were harvested at 24 h intervals, and the recovered DNA was electrophoresed on 1% agarose gels with a standard marker (*M*). An increase in the sub-G_1 peak was evident by 72 h, which was accompanied by DNA laddering. The data presented are representative of three independent experiments.

Table 1 Cell cycle analysis of glioblastoma cell lines with and without flavopiridol treatment

Time (h)	Phase	A172 (wt)[a]		U87MG (wt)		T98G (mu)		U118MG (mu)	
		Control	Flavo	Control	Flavo	Control	Flavo	Control	Flavo
0	Sub-G_1	3.46	2.5	4.72	4.31	9.61	5.05	8.65	3.24
	G_0-G_1	67.78	70.52	40.23	43.09	48.6	49.16	75.06	75.25
	S	26.09	24.78	57.45	55.11	46.09	44.66	15.94	15.36
	G_2-M	5.65	4.69	2.32	1.8	5.3	6.18	9	9.38
24	Sub-G_1	2.92	15.43	1.75	8.91	5.6	13.45	10.93	15.45
	G_0-G_1	66.8	63.07	57.68	43.01	47.87	39.38	48.6	58.18
	S	23.24	25.01	27.38	12.28	43.53	16.3	31.81	28.07
	G_2-M	9.95	11.92	14.94	44.71	8.6	44.32	19.59	13.76
48	Sub-G_1	2.86	28.51	2.26	8.62	2.32	23.59	7.34	12.34
	G_0-G_1	72.48	62.68	77.77	44.14	54.62	38.79	62.25	54.18
	S	18.31	23.41	13.83	7.76	36.16	16.74	22.38	25.67
	G_2-M	9.21	13.92	8.4	48.1	9.22	45.07	15.36	20.14
72	Sub-G_1	3.84	34.26	3.25	22.18	3.06	34.51	5	25.38
	G_0-G_1	59.95	70.17	84.32	46.3	64	42.83	61.62	57.54
	S	30.92	16.22	12.07	10.44	28.76	20.97	25.23	25.22
	G_2-M	9.13	13.61	27.64	27	7.25	36.2	13.13	17.24

[a] wt, wild-type p53; mu, mutant p53; flavo, flavopiridol-treated cells.

treatment in all of the cell lines. Two markers of apoptosis, caspase 3 and PARP, were evaluated. In all wild-type and mutant p53 cell lines treated with flavopiridol, no cleavage products of caspase 3 or PARP protein were observed. Cells treated with the pan-caspase inhibitor Z-VAD-fmk in combination with flavopiridol showed similar patterns of protein expression as cells treated with flavopiridol alone (data not shown).

Flavopiridol-mediated Apoptosis Is Caspase Independent. To further explore the mechanism of caspase-independent cell death observed in flavopiridol-treated glioma cell lines, we compared the effects of flavopiridol on the HL-60 promyelocytic leukemia cell line as a positive control. HL-60 cells are sensitive to flavopiridol treatment and readily demonstrate caspase 3 activation, PARP, and caspase 8 cleavage (25–28). Similarly, in our hands, HL-60 cells treated with 200 nM flavopiridol showed caspase 3, PARP, and caspase 8 cleavage products beginning at 2 h, which was completely inhibited by pretreatment with the pan-caspase inhibitor Z-VAD-fmk (data not shown). Next, we reevaluated the cleavage of the same three markers for apoptosis in one representative glioma cell line, A172, treated for up to 72 h with 300 nM flavopiridol (Fig. 5). Western blots containing lysates from HL-60 cells treated with flavopiridol for 4 h (Fig. 5, *Lane C*) together with lysates from A172 cells treated with flavopiridol for different time intervals were probed with the appropriate antibodies. Once again, HL-60 samples treated with flavopiridol clearly demonstrated the signature cleavage products for caspase 3 activation (M_r 17,000), PARP (M_r 85,000), and caspase 8 (M_r 18,000) cleavage that were undetectable in the A172 drug-treated cultures. Taken together,

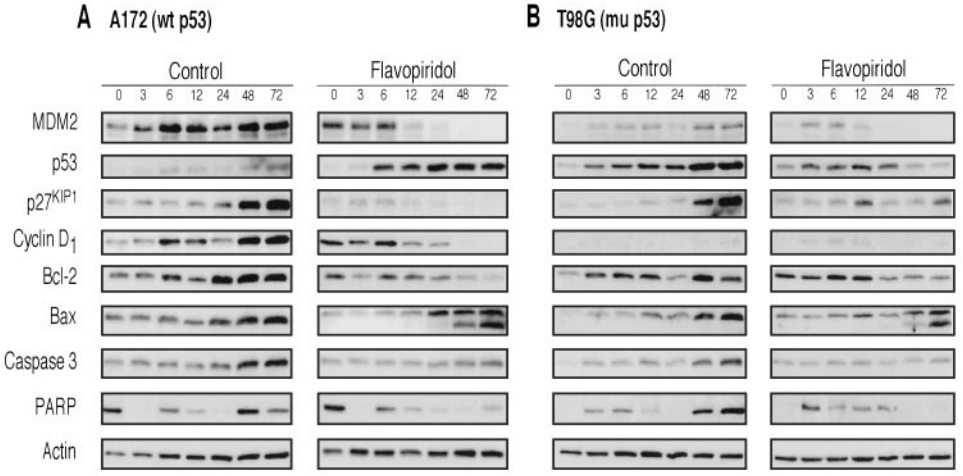

Fig. 4. Flavopiridol induced changes in the expression of cell cycle proteins. Changes in the expression of various cell cycle proteins were analyzed by Western blotting. Representative data are shown for the A172 cell line expressing wild-type (*wt*) p53 (*A*) and the T98G cell line expressing mutant (*mu*) p53 (*B*). Total cells untreated or treated with 300 nM flavopiridol were harvested at the appropriate time interval, lysed, and equal amounts of protein (30 μg) were electrophoresed on 7.5 or 12% SDS-PAGE gels. Immunoblotting was performed with antibodies to the respective proteins. PARP expression was assessed using a mouse monoclonal antibody (C2–10; PharMingen). The data presented are representative of three independent experiments.

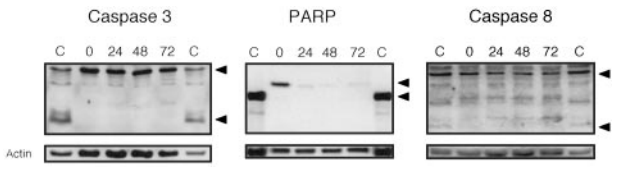

Fig. 5. Flavopiridol-mediated apoptosis is caspase independent. Representative data are shown for the glioma A172 cell line expressing wild-type p53. Total cells untreated or treated with 300 nM flavopiridol were harvested at 24 h time intervals, lysed, and equal amounts of protein (30 μg) were electrophoresed on 7.5 or 12% SDS-PAGE gels. Immunoblotting was performed with antibodies to the respective proteins. The promyelocytic leukemia HL-60 cell line treated with 200 nM flavopiridol for 4 h served as a positive control (C) for caspase 3 activation, PARP, and caspase 8 cleavages. *Arrowheads* denote the proform and the cleavage products. The data presented are representative of three independent experiments.

these findings suggest that flavopiridol induces apoptosis by a caspase-independent pathway in human glioma cells compared with a caspase-dependent pathway in human HL-60 promyelocytic leukemia cells.

Flavopiridol-mediated Apoptosis Occurs without Cytochrome *c* Release but Induces AIF Translocation. Mitochondrial damage occurring as a result of drug-induced apoptosis is often accompanied by release of cytochrome *c* from the mitochondria into the cytosol (10, 26, 28, 29). Because flavopiridol treatment induced caspase-dependent apoptosis in HL-60 cells, we investigated cytochrome *c* release in these cells as a positive control using immunohistochemical methods as previously reported (29). Untreated HL-60 cells demonstrated cytochrome *c* staining in a punctate pattern indicating its normal location in mitochondria together with normal nuclear morphology, whereas HL-60 cells treated with flavopiridol showed an increased diffuse staining of cytochrome *c* in the cytoplasm, which was accompanied by chromatin condensation and nuclear fragmentation typical of apoptosis (data not shown). To determine whether flavopiridol induced similar changes in mitochondria of A172 cells, the glioma cells were untreated or treated for different time intervals with 300 nM flavopiridol and the pattern of cytochrome *c* immunostaining examined using fluorescence microscopy (Fig. 6, *A* and *B*). Untreated A172 glioma cells showed normal nuclear morphology by DAPI staining (blue fluorescence) and a distinct punctate pattern of cytochrome *c* immunostaining (green fluorescence) that was located largely in a perinuclear ring (Fig. 6*A*), similar to the pattern observed in untreated HL-60 cells. Cultures of A172 cells treated with the drug for up to 72 h (Fig. 6*B*) retained normal nuclear morphology by DAPI staining and demonstrated a cytochrome *c* immunostaining pattern similar to that observed in untreated cells. These findings indicated that apoptosis induced by flavopiridol in glioma cells occurs in the absence of cytochrome *c* release.

Other proteins are also associated with mitochondria and released during apoptosis. AIF is another apoptotic regulatory protein that translocates from the mitochondria to the nucleus and its subcellular location can be detected by immunofluorescence similar to the redistribution of cytochrome *c* from the mitochondria to the cytosol. Untreated A172 glioma cells showed normal nuclear morphology by DAPI staining (blue fluorescence) and a distinct punctate pattern of AIF immunostaining (red fluorescence), indicating its normal location in the mitochondria (Fig. 6*C*). Cultures of A172 cells treated with the drug for 72 h (Fig. 6*D*) demonstrated a more diffuse and nuclear immunostaining pattern indicating the translocation of AIF into the nucleus. These findings taken together indicated that apoptosis induced by flavopiridol in glioma cells occurs via the release of AIF.

Transmission Electron Microscopy of Flavopiridol-treated A172 Glioma Cells. To further investigate the mechanisms of flavopiridol-induced cytotoxicity, ultrastructural characteristics of apoptosis were examined by trans-

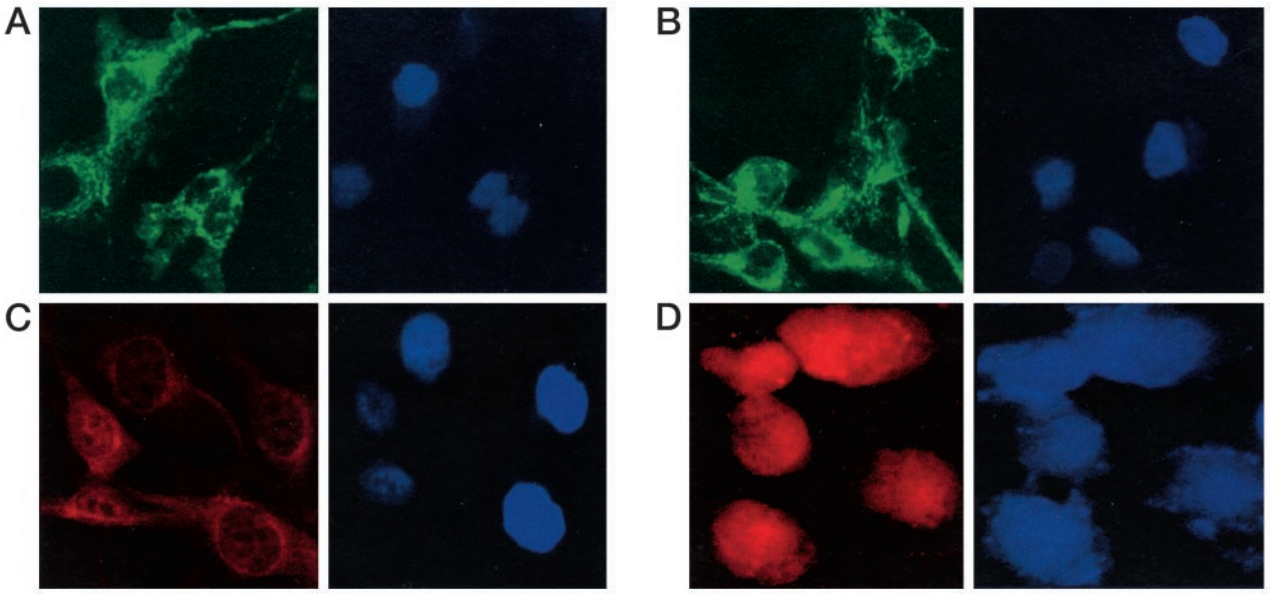

Fig. 6. Flavopiridol-mediated apoptosis occurs without cytochrome *c* release but induces AIF translocation. The A172 glioma cell line was untreated (*A* and *C*) or treated with 300 nM flavopiridol for 72 h (*B* and *D*), and the pattern of cytochrome *c* (*A* and *B*) or AIF (*C* and *D*) staining was examined using fluorescence microscopy. Cells were fixed and permeabilized, followed by immunostaining with an antiserum specific for cytochrome *c* (*green fluorescence*) or AIF (*red fluorescence*) and counterstaining with DAPI (*blue fluorescence*) to visualize nuclear morphology. In the A172 glioma cells that undergo caspase-independent apoptosis, no changes in the cytochrome *c* immunofluorescence was observed in flavopiridol treated for 72 h (*B*) compared with untreated cells (*A*). In contrast, the A172 glioma cells stained for AIF showed a redistribution of AIF from the mitochondria to the nucleus (*D*) induced by flavopiridol treatment for 72 h compared with the control (*C*). The data presented are representative of three independent experiments.

mission electron microscopy (Fig. 7). Because maximal cytotoxicity was observed in A172 cells treated with flavopiridol for 72 h, this time point was selected for evaluation of ultrastructural changes induced by drug treatment.

Transmission electron microscopy of untreated cultures (Fig. 7*A*) showed healthy cells with irregularly round cell bodies and numerous fine surface microvillar processes. The nuclei were distinctly convoluted and even segmented but had mostly euchromatic contents. In comparison, the cells in the drug-treated culture showed many with mild or marked vacuolation of the cytoplasm (Fig. 7, *B–D*) with the vacuoles bounded by a single layer of membrane and containing various amounts of membranous debris. In some cells with an early form of this change, the vacuoles appeared to represent dilated portions of endoplasmic reticulum. In other cells, it was clear that the vacuoles represented or included secondary lysosomes (Fig. 7*D*). Most of the vacuolated cells had nuclei similar to those observed in the untreated cells (Fig. 7*D*). However, other cells without vacuolation had nuclear changes, including marked condensation of chromatin, collapse of nuclei, and nuclear fragmentation (Fig. 7, *B* and *C*). A few cells showed both the cytoplasmic vacuolation and the nuclear damage (Fig. 7*B*). In both populations of untreated and treated cells, numerous mitochondria were detected that appeared ultrastructurally normal, *i.e.,* no swelling or displacement of cristae or other abnormalities. Whether any of the vacuolation in the drug-treated cells is attributable to mitochondrial swelling is unclear but appears unlikely because the vacuoles lacked double membranes or detectable cristae, which are characteristic of mitochondria. These findings taken together with the cytochrome *c* data indicate that flavopiridol exerts its cytotoxic effects in glioma cells in the absence of detectable mitochondrial damage.

Flavopiridol Did Not Change the Half-Life of MDM2. Unexpectedly, flavopiridol treatment of glioma cells led to the marked depletion of MDM2 protein expression within 12 h. Therefore, we wanted to determine the basis for this loss of MDM2 protein expression. Changes in protein degradation can be measured by determining the level of a protein at various time intervals after treatment with an inhibitor of protein synthesis such as cycloheximide. Cycloheximide was added to cultures of the A172 cell line expressing wild-type p53 and the T98G cell line expressing mutant p53 untreated or pretreated with 300 nM flavopiridol for 6 h (Fig. 8). The half-life of MDM2 was determined to be <1 h regardless of *p53* status or the presence or absence of flavopiridol. As a control, we measured the half-life of the p53 protein in the same cultures. As expected, cycloheximide treatment stabilized the levels of p53 protein in the A172 cell line expressing wild-type p53 but had no effect on the levels of p53 protein in the T98G cell line expressing mutant p53 (Fig. 8). The half-life of cyclin D_1 did not change in the presence of flavopiridol (data not shown).

Flavopiridol Decreased MDM2 mRNA Levels. Because flavopiridol treatment did not change the half-life of the MDM2 protein, we assessed whether gene transcription was altered after drug treatment. The steady-state levels of mRNA were measured by Northern blot analysis. Representative data are shown for the A172 cell line expressing wild-type p53 and the T98G cell line expressing mutant p53 (Fig.

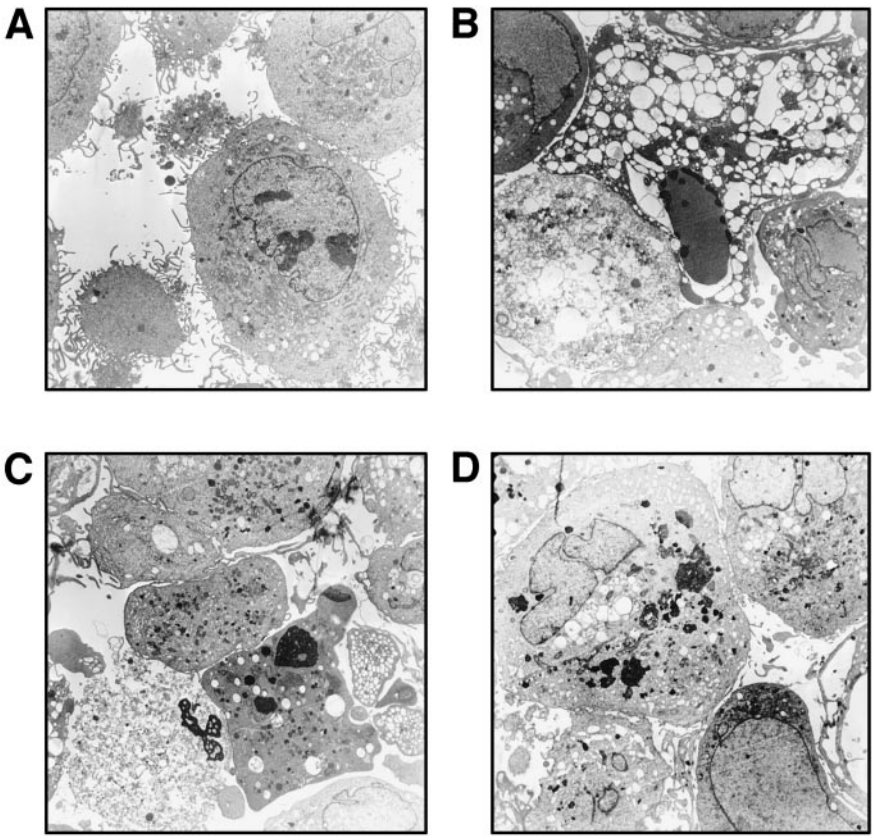

Fig. 7. Transmission electron microscopy of cultured A172 glioma cells. The A172 glioma cell line was untreated (*A*) or treated with 300 nM flavopiridol for 72 h (*B–D*), and total cells were harvested and processed for transmission electron microscopy. *A*, untreated cells are each irregularly round with large nuclei; the nuclei are mostly euchromatic and often convoluted or even segmented (see cell in *top right corner*). The cell surface has numerous microvillar projections, and the cytoplasm has numerous mitochondria with detectable cristae and a well-developed endoplasmic reticulum. There are occasional vacuoles in the cytoplasm. *B*, some of the cells treated with flavopiridol for 72 h are relatively well-preserved, with nuclei indistinguishable from untreated controls (see cell in *bottom right corner*) and with only a modest increase in cytoplasmic vacuoles, some of which now contain membranous debris (secondary lysosomes). Other cells are markedly abnormal with massive cytoplasmic vacuolation. One of these cells (occupying most of the *top half of the figure*) has a nucleus with dense nucleoplasm with small clumps of residual chromatin at the inner border of the nuclear membrane. *C*, in the bottom half of this electron micrograph are two cells, the nuclei of which have fragmented into multiple clumps of dense chromatin. In the affected cell to the *left* the nuclei has a lobated or segmented appearance typical of apoptotic nuclear destruction. The cytoplasm of both cells is vacuolated with considerable loss of organelles, although normal residual mitochondria are present in the less damaged cell to the *right*. *D*, these cells have nuclei that retain the appearance of those observed in untreated cells. Some vacuoles present in the cytoplasm are derived from expanded cisternae of the endoplasmic reticulum, and there is also dense membranous debris in secondary lysosomes. Numerous mitochondria are present that appear ultrastructurally normal, *i.e.,* they have no swelling or displacement of the cristae or other abnormalities. Original magnification: ×5000.

9). For A172, there was a 2-fold decrease in MDM2 mRNA transcript levels by 6 h of drug treatment, which then became undetectable at 12 h compared with the 0 h time point. p53 and cyclin D_1 mRNA transcript levels appeared to be transiently up-regulated at 6 h of drug treatment compared with control cultures at 0 and 6 h. Thereafter, the p53 and cyclin D_1 mRNA transcript levels decreased becoming barely detectable at 24 h of drug treatment. For T98G, MDM2 mRNA transcript levels were undetectable at 6 h of drug treatment, whereas p53 and cyclin D_1 mRNA transcript levels remained at a low level throughout the 24-h interval.

Discussion

We have shown two novel findings in glioma cell lines treated with flavopiridol. First, flavopiridol induces apoptosis through a caspase-independent mechanism in all of the glioma cell lines. Second, flavopiridol decreased expression of both MDM2 mRNA and protein by 24 h in all of the cell lines independent of Rb or p53 tumor suppressor pathway alterations.

Using our panel of six glioma cell lines, we demonstrated that apoptosis induced by flavopiridol was independent of Rb and p53 alterations in agreement with previous reports in leukemia, lung, breast, and gastric tumor cell lines (18, 27, 30–32). In contrast to the reports of others who tested flavopiridol in these other cell lines, flavopiridol-induced apoptosis in this study of glioma cell lines was not accompanied by activation of caspase 3 or cleavage of PARP and caspase 8 in the glioma cell lines (18, 28, 32, 33). Similarly, addition of the pan-caspase inhibitor Z-VAD-fmk did not inhibit drug-induced apoptosis as measured by decreased cell viability, DNA laddering, and appearance of a sub-G_1 peak in cell cycle analysis nor did it alter changes in protein expression in any of the

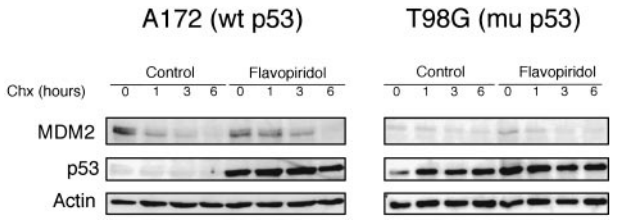

Fig. 8. Flavopiridol did not change the half-life of MDM2. Changes in protein degradation were measured by determining the level of a protein at various time intervals after treatment with the protein synthesis inhibitor cycloheximide (*Chx*). Representative data are shown for the A172 cell line expressing wild-type (*wt*) p53 and the T98G cell line expressing mutant (*mu*) p53. Cycloheximide (100 μg/ml) was added to cultures untreated or pretreated with 300 nM flavopiridol for 6 h. Total cells were harvested from each culture condition at the appropriate time interval (in hours), washed, and subjected to lysis and protein extraction for Western blotting. The data presented are representative of three independent experiments.

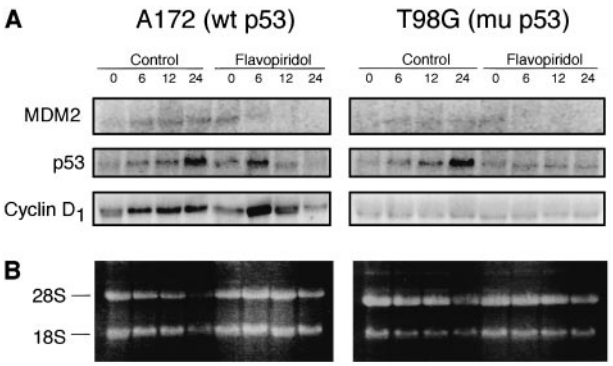

Fig. 9. Flavopiridol decreased MDM2 mRNA levels. The steady-state mRNA transcript levels were measured by Northern blot analysis. Representative data are shown for the A172 cell line expressing wild-type (wt) p53 and the T98G cell line expressing mutant (mu) p53 (*A*). RNase, 28S and 18S, is shown for equal loading (*B*). mRNA transcript levels were measured in cells untreated and treated with 300 nM flavopiridol for 24 h. Total cellular RNA was isolated from the cell cultures at the appropriate time interval and resolved on a formaldehyde gel. The membranes were probed sequentially for MDM2, p53, and cyclin D_1. The MDM2 mRNA transcript levels decreased by 6 h with flavopiridol treatment in both A172 and T98G cell lines. The data presented are representative of two independent experiments.

drug-treated cells (data not shown). To further examine the basis of flavopiridol-induced cytotoxicity, we assessed the status of mitochondria in untreated and treated cell cultures using cytochrome *c*, AIF immunohistochemistry, and transmission electron microscopy. The staining pattern for cytochrome *c* remained punctate and perinuclear in both the untreated and treated cells over the 72-h interval of drug treatment. This finding suggested that mitochondria remained largely intact because the release of cytochrome *c* into the cytosol would have produced a diffuse staining pattern as we observed in flavopiridol treated HL-60 cells (data not shown). The ultrastructural data obtained with transmission electron microscopy additionally supported this conclusion that mitochondria remained structurally intact in glioma cells treated with flavopiridol. Taken together, these results suggest that apoptosis in glioma cell lines may be mediated through a caspase-independent mechanism. Recent genetic evidence shows that there is a caspase-independent pathway of programmed cell death involving AIF (34–36). Most recently, an AIF-homologous mitochondrion-associated inducer of death protein was cloned and characterized and was shown to also induce caspase-independent apoptosis (37). Both AIF and AIF-homologous mitochondrion-associated inducer of death are localized to the mitochondria, similar to cytochrome *c*, and both are released in response to death stimuli to induce caspase-independent apoptosis, neither of which can be inhibited by the pan-caspase inhibitor Z-VAD-fmk. Using AIF immunohistochemistry, we show that apoptosis induced by flavopiridol in glioma cells occurs via the release of AIF and its translocation from the mitochondria to the nucleus.

We observed that flavopiridol treatment consistently down-regulated MDM2 expression in all six glioma lines independent of *p53* status or levels of MDM2 expression. Loss of MDM2 expression was not because of increased degradation of the protein upon addition of flavopiridol because cycloheximide treatment did not affect the half-life of the MDM2 protein. Instead, loss of MDM2 expression was because of decreased mRNA transcript levels detectable within 6 h of drug treatment. A decrease in gene transcription rather than an increase in degradation of the protein has been reported for cyclin D_1 in response to flavopiridol treatment (19). Thus, one mechanism of action of flavopiridol may be to alter transcript levels encoding proteins rather than to increase degradation of these proteins. These results are consistent with the reports that flavopiridol plays a major role in the regulation of gene transcription via its ability to inactivate the positive transcription elongation factor b (38). In particular, flavopiridol appears to affect the transcription of genes that have short mRNA half-lives, a characteristic of both the MDM2 and cyclin D_1 genes (39, 40).

Negative regulation of p53 by MDM2 is essential in cell cycle control. MDM2 inactivates p53 expression in two ways: (*a*) by binding to its transactivation domain; and (*b*) by targeting p53 for degradation (41, 42). Overexpression of MDM2 occurs in a variety of human tumors via different mechanisms including gene amplification, increased transcription, or enhanced translation (41–43). In GBM, we have noted overexpression of MDM2 in >50% of adult tumors in the absence of gene amplification (6, 7). In addition, overexpression of MDM2 in some glioma cell lines has been associated with drug resistance (8, 9).

Previous work in glioma cell lines expressing wild-type p53, using antisense oligodeoxynucleotides to MDM2, showed that a decrease in MDM2 mRNA levels was associated with a decrease in MDM2 protein expression and, additionally, that this resulted in increased chemosensitivity to cisplatin, paclitaxel, and irinotecan both *in vitro* and *in vivo* (8, 44). Antisense MDM2 treatment in cell lines with either an amplified MDM2 gene or overexpression of MDM2 was associated with decreased MDM2-p53 complex formation, increased p53-inducible gene expression, increased p53 transcriptional activity, and apoptosis (9). Similarly, flavopiridol treatment of glioma cell lines expressing wild-type p53 induced a loss of MDM2 protein, which was associated with an

increase in p53 protein levels, while p53 mRNA transcript levels decreased. This is expected because wild-type p53 protein would become stabilized because of loss of MDM2-targeted degradation of p53. Thus, flavopiridol treatment should promote increased p53 activity similar to that observed after MDM2 antisense treatment of glioma cell lines (8, 9, 44, 45).

MDM2 may have gain-of-function activities. There is evidence to suggest that overexpression of MDM2 may impart tumorigenic properties. First, adults with soft tissue sarcomas that have both overexpression of MDM2 and mutations in *p53* have a significantly worse prognosis than those individuals with tumors having only one alteration (46). Second, transgenic mice with increased MDM2 expression in a *p53*-null background had an increased incidence of sarcomas (47). In addition, several human tumor cell lines expressing wild-type p53 but with MDM2 amplification or overexpression at the same time have a functional p53 response (stabilization of p53, activation of p53-inducible genes, and cell cycle arrest) to DNA damaging agents (41). Taken together, these results suggest that overexpression of MDM2 may have tumor-promoting activity independent of p53. In this study, we found that in glioma cell lines with mutant p53, loss of MDM2 protein was not accompanied by changes in p53 protein expression or mRNA transcript levels. This is expected because mutant p53 proteins are already highly stable (48). However, by decreasing the cellular levels of MDM2, flavopiridol treatment may serve to reduce any growth advantages conferred by oncogenic activities associated with the MDM2 protein. Taken together, our results suggest that flavopiridol may be effective in treating GBMs expressing either wild-type or mutant p53 proteins.

In our study, cyclin D_1 as well as MDM2 protein levels decrease early after flavopiridol treatment. By decreasing cyclin D_1 protein levels, CDK4 kinase activity is decreased, which results in the accumulation of hypophosphorylated Rb that favors growth arrest. Because >80% of GBMs have alterations in the Rb tumor suppressor pathway via $p16^{INK4a}$ gene deletion, amplification of CDK4, or mutation in Rb, flavopiridol may prove to be an effective chemotherapeutic agent for GBM.

We noted that Bcl-2 protein expression became down-regulated 24 and 48 h after drug treatment, whereas Bax protein levels were up-regulated in all of the cell lines during the same time interval resulting in a low Bcl-2/Bax ratio. We have previously reported that a high Bcl-2/Bax ratio of protein expression was associated with drug resistance (49). The Bcl-2 family consists of both proapoptotic proteins (*e.g.,* Bax) and antiapoptotic proteins (*e.g.,* Bcl-2) that form homodimers or heterodimers (50, 51). Formation of heterodimers of antiapoptotic proteins with proapoptotic proteins can neutralize the effect of antiapoptotic proteins. Thus, the ratio of antiapoptotic proteins to proapoptotic proteins can determine whether the cell will survive or undergo apoptosis (50–52). Because flavopiridol treatment results in a low Bcl-2/Bax ratio in glioma cell lines, this may be one mechanism for inducing apoptosis.

In summary, we have examined the effect of flavopiridol on a panel of glioma cell lines with genetic alterations in both the Rb and p53 tumor suppressor pathways. Regardless of the genetic makeup, flavopiridol induced growth arrest in most of the cell lines by 24 h. Drug-induced apoptosis occurred by 72 h in all of the cell lines through a caspase-independent mechanism. We also observed that flavopiridol reduced MDM2 mRNA transcripts and produced a complete loss of MDM2 protein in all of the cell lines. Given that MDM2 protein can regulate Rb and p53 function as well as confer oncogenic properties under certain circumstances, loss of MDM2 expression in tumor cells could promote increased chemosensitivity. Studies on flavopiridol in combination with other therapeutic drugs such as mitomycin, cytarabine, paclitaxel, and cisplatin have shown to have a synergistic effect only when the cells are first pretreated with flavopiridol for 24 h (53–55). From our study, at 24 h of flavopiridol treatment, wild-type p53 is at its maximal potential for activity because of loss of MDM2 protein expression. Therefore, introduction of a DNA damaging agent at this point allows the agent to have an increased effectiveness in inducing apoptosis. Reduction of MDM2 mRNA described here may be the basis of this effect. In future studies, we will examine the effect of flavopiridol treatment in combination with other chemotherapeutic agents on glioma cell lines. Taken together, the data indicates that flavopiridol has activity against GBM cell lines *in vitro* and should be considered for clinical development in the treatment of GBM.

Acknowledgments

We thank Dr. Robert B. Carroll for helpful discussion and advice.

References

1. Sherr, C. J. The INK4a/ARF network in tumour suppression. Nat. Rev., *2:* 731–737, 2001.

2. Kleihues, P., Burger, P. C., Collins, P., Newcomb, E. W., Ohgaki, H., and Cavenee, W. K. Glioblastoma. *In*: P. Kleihues and W. K. Cavenee (eds.), Pathology and Genetics of Tumours of the Nervous System, pp. 29–39. Lyon, France: IARC Press, 2000.

3. Louis, D. N., Holland, E. C., and Cairncross, J. G. Glioma classification: a molecular reappraisal. Am. J. Pathol., *159:* 779–786, 2001.

4. Levine, A. J. p53, the cellular gatekeeper for growth and division. Cell, *88:* 323–331, 1997.

5. Balint, E., and Vousden, K. H. Activation and activities of the p53 tumour suppressor protein. Br. J. Cancer, *85:* 1813–1823, 2001.

6. Lang, F. F., Miller, D. C., Koslow, M., and Newcomb, E. W. Pathways leading to glioblastoma multiforme: a molecular analysis of genetic alterations in 65 astrocytic tumors. J. Neurosurg., *81:* 427–436, 1994.

7. Newcomb, E. W., Cohen, H., Lee, S. R., Bhalla, S. K., Bloom, J., Hayes, R. L., and Miller, D. C. Survival of patients with glioblastoma multiforme is not influenced by altered expression of p16, p53, EGFR, MDM2, or Bcl-2 genes. Brain Pathol., *8:* 655–667, 1998.

8. Kondo, S., Barnett, G. H., Hara, H., Morimura, T., and Takeuchi, J. MDM2 protein confers the resistance of a human glioblastoma cell line to cisplatin-induced apoptosis. Oncogene, *10:* 2001–2006, 1995.

9. Chen, L., Agrawal, S., Zhou, W., Zhang, R., and Chen, J. Synergistic activation of p53 by inhibition of MDM2 expression and DNA damage. Proc. Natl. Acad. Sci. USA, *95:* 195–200, 1998.

10. Johnstone, R. W., Ruefli, A. A., and Lowe, S. W. Apoptosis: A link between cancer genetics and chemotherapy. Cell, *108:* 153–164, 2002.

11. Sherr, C. J., and Weber, J. D. The ARF/p53 pathway. Curr. Opin. Genet. Dev., *10:* 94–99, 2000.

12. Naik, R. G., Kattige, S. L., Bhat, S. B., Alreja, B., De Souza, N. J., and Rupp, R. H. An anti-inflammatory cum immunomodulatory piperidinylbenzopyranone from Dysoxylum binectariferum: isolation, structure, and total synthesis. Tetrahedron, *44:* 2081–2086, 1988.

13. Senderowicz, A. M., Headlee, D., Stinson, S. F., Lush, R. M., Kalil, N., Villalba, L., Hill, K., Steinberg, S. M., Figg, W. D., Tompkins, A., Arbuck, S. G., and Sausville, E. A. Phase I trial of continuous infusion flavopiridol, a novel cyclin-dependent kinase inhibitor, in patients with refractory neoplasms. J. Clin. Oncol., *16:* 2986–2999, 1998.

14. Senderowicz, A. M. Flavopiridol: the first cyclin-dependent kinase inhibitor in human clinical trials. Investig. New Drugs, *17:* 313–320, 1999.

15. Kelland, L. R. Flavopiridol, the first cyclin-dependent kinase inhibitor to enter the clinic: current status. Exp. Opin. Investig. Drugs, *9:* 2903–2911, 2000.

16. Schwartz, G. K., Ilson, D., Saltz, L., O'Reilly, E., Tong, W., Maslak, P., Werner, J., Perkins, P., Stoltz, M., and Kelsen, D. Phase II study of the cyclin-dependent kinase inhibitor flavopiridol administered to patients with advanced gastric carcinoma. J. Clin. Oncol., *19:* 1985–1992, 2001.

17. Stadler, W. M., Vogelzang, N. J., Amato, R., Sosman, J., Taber, D., Liebowitz, D., and Vokes, E. E. Flavopiridol, a novel cyclin-dependent kinase inhibitor, in metastatic renal cancer: a University of Chicago Phase II consortium study. J. Clin. Oncol., *18:* 371–375, 2000.

18. Sedlacek, H. H. Mechanisms of action of flavopiridol. Crit. Rev. Oncol. Hematol., *38:* 139–170, 2001.

19. Carlson, B., Lahusen, T., Singh, S., Loaiza-Perez, A., Worland, P. J., Pestell, R., Albanese, C., Sausville, E. A., and Senderowicz, A. M. Down-regulation of cyclin D_1 by transcriptional repression in MCF-7 human breast carcinoma cells induced by flavopiridol. Cancer Res., *59:* 4634–4641, 1999.

20. Ishii, N., Maier, D., Merlo, A., Tada, M., Sawamura, Y., Diserens, A-C., and Van Meir, E. G. Frequent co-alterations of TP53, p16/CDKN2A, $p14^{ARF}$, PTEN tumor suppressor genes in human glioma cell lines. Brain Pathol., *9:* 469–479, 1999.

21. Newcomb, E. W., Alonso, M., Sung, T., and Miller, D. C. Incidence of $p14^{ARF}$ gene deletion in high-grade adult and pediatric astrocytomas. Hum. Pathol., *31:* 115–119, 2000.

22. Hunter, S. B., Abbott, K., Varma, V. A., Olson, J. J., Barnett, D. W., and James, C. D. Reliability of differential PCR for the detection of EGFR and MDM2 gene amplification in DNA extracted from FFPE glioma tissue. J. Neuropath. Exp. Neurol., *54:* 57–64, 1995.

23. Wood, D. E., Thomas, A., Devi, L. A., Berman, Y., Beavis, R. C., Reed, J. C., and Newcomb, E. W. Bax cleavage is mediated by calpain during drug-induced apoptosis. Oncogene, *17:* 1069–1078, 1998.

24. Schmid, I., Uittenbogaart, C. H., and Giorgi, J. V. Sensitive method for measuring apoptosis and cell surface phenotype in human thymocytes by flow cytometry. Cytometry, *15:* 12–20, 1994.

25. Bible, K. C., and Kaufmann, S. H. Flavopiridol: a cytotoxic flavone that induces cell death in noncycling A549 human lung carcinoma cells. Cancer Res., *56:* 4586–4861, 1996.

26. Arguello, F., Alexander, M., Sterry, J. A., Tudor, G., Smith, E. M., Kalavar, N. T., Greene, J. F., Koss, W., Morgan, C. D., Stinson, S. F., Siford, T. J., Alvord, W. G., Klabansky, R. L., and Sausville, E. A. Flavopiridol induces apoptosis of normal lymphoid cells, causes immunosuppression, and has potent antitumor activity *in vivo* against human leukemia and lymphoma xenografts. Blood, *91:* 2482–2490, 1998.

27. Rapoport, A. P., Simons-Evelyn, M., Chen, T., Sidell, R., Luhowskyj, S., Rosell, K., Obrig, T., Hicks, D., Hinkle, P. M., Nahm, M., Insel, R. A., and Abboud, C. N. Flavopiridol induces apoptosis and caspase-3 activation of a newly characterized Burkitt's lymphoma cell line containing mutant p53 genes. Blood Cells Mol. Dis., *27:* 610–624, 2001.

28. Rosato, R. R., Almenara, J. A., Cartee, L., Betts, V., Chellappan, S. P., and Grant, S. The cyclin-dependent kinase inhibitor flavopiridol disrupts sodium butyrate-induced p21 WAF1/CIP1 expression and maturation while reciprocally potentiating apoptosis in human leukemia cells. Mol. Cancer Ther., *1:* 253–266, 2002.

29. Gruss-Fischer, T., and Fabian, I. Protection by ascorbic acid from denaturation and release of cytochrome *c*, alteration of mitochondrial membrane potential and activation of multiple caspases induced by H_2O_2, in human leukemic cells. Biochem. Pharmacol., *63:* 1325–1335, 2002.

30. Shapiro, G. I., Koestner, D. A., Matranga, C. B., and Rollins, B. J. Flavopiridol induces cell cycle arrest and p53-independent apoptosis in non-small cell lung cancer cell lines. Clin. Cancer Res., *5:* 2925–2938, 1999.

31. Lu, K., Shih, C., and Teicher, B. A. Expression of pRB, cyclin/cyclin-dependent kinases and E2F1/DP-1 in human tumor lines in cell culture and in xenograft tissues and response to cell cycle agents. Cancer Chemother. Pharmacol., *46:* 293–304, 2000.

32. Byrd, J. C., Shinn, C., Waselenko, J. K., Fuchs, E. J., Lehman, T. A., Nguyen, P. L., Flinn, I. W., Diehl, L. F., Sausville, E. A., and Grever, M. R. Flavopiridol induces apoptosis in chronic lymphocytic leukemia cells via activation of caspase-3 without evidence of bcl-2 modulation or dependence on functional p53. Blood, *92:* 3804–3816, 1998.

33. Motwani, M., Delohery, T. M., and Schwartz, G. K. Sequential dependent enhancement of caspase activation and apoptosis by flavopiridol on paclitaxel-treated human gastric and breast cancer cells. Clin. Cancer Res., *5:* 1876–1883, 1999.

34. Susin, S. A., Lorenzo, H. K., Zamzami, N., Marzo, I., Snow, B. E., Brothers, G. M., Mangion, J., Jacotot, E., Constantini, P., Loeffler, M., Larochette, N., Goodlett, D. R., Aebersold, R., Siderovski, D. P., Penninger, J. M., and Kroemer, G. Molecular characterization of mitochondrial apoptosis-inducing factor. Nature (Lond.), *397:* 441–446, 1999.

35. Daugas, E., Susin, S. A., Zamzami, N., Ferri, K. F., Irinopoulou, T., Larochette, N., Prevost, M. C., Leber, B., Andrews, D., Penninger, J., and Kroemer, G. Mitochondrio-nuclear translocation of AIF in apoptosis and necrosis. FASEB J., *14:* 729–739, 2000.

36. Cregan, S. P., Fortin, A., MacLaurin, J. G., Callaghan, S. M., Cecconi, F., Yu, S-W., Dawson, T. M., Dawson, V. L., Park, D. S., Kroemer, G., and Slack, R. S. Apoptosis-inducing factor is involved in the regulation of caspase-independent neuronal cell death. J. Cell Biol., *158:* 507–517, 2002.

37. Wu, M., Xu, L-G., Li, X., Zhai, Z., and Shu, H-B. AMID, an apoptosis-inducing factor-homologous mitochondrion-associated protein, induces caspase-independent apoptosis. J. Biol. Chem., *277:* 25617–25623, 2002.

38. Chao, S-H., and Price, D. H. Flavopiridol inactivates P-TEFb and blocks most RNA polymerase II transcription *in vivo*. J. Biol. Chem., *276:* 31793–31799, 2001.

39. Lam, L. T., Pickeral, O. K., Peng, A. C., Rosenwald, A., Hurt, E. M., Giltnane, J. M., Averett, L. M., Zhao, H., Davis, R. E., Sathyamoorthy, M., Wahl, L. M., Harris, E. D., Mikovits, J. A. Monks, A. P., Hollingshead, M. G., Sausville, E. A., and Staudt, L. M. Genomic-scale measurement of mRNA turnover and the mechanisms of action of the anti-cancer drug flavopiridol. Genome Biol., *2:* 1–11, 2001.

40. Sausville, E. A. Complexities in the development of cyclin-dependent kinase inhibitor drugs. Trends Mol. Med., *8:* 32–37, 2002.

41. Freedman, D. A., Wu, L., and Levine, A. J. Functions of the MDM2 oncoprotein. Cell. Mol. Life Sci., *55:* 96–107, 1999.

42. Alarcon-Vargas, D., and Ronai, Z. p53-Mdm2: the affair that never ends. Carcinogenesis (Lond.), *23:* 541–547, 2002.

43. Landers, J. E., Cassel, S. L., and George, D. L. Translational enhancement of mdm2 oncogene expression in human tumor cells containing a stabilized wild-type p53 protein. Cancer Res., *57:* 3562–3568, 1997.

44. Prasad, G., Wang, H., Agrawal, S., and Zhang, R. Antisense anti-MDM2 oligonucleotides as a novel approach to the treatment of glioblastoma multiforme. Anticancer Res., *22:* 107–116, 2002.

45. Inoue, T., Geyer, R. K., Yu, Z. K., and Maki, C. G. Down-regulation of MDM2 stabilizes p53 by inhibiting p53 ubiquitination in response to specific alkylating agents. FEBS Lett., *490:* 196–201, 2001.

46. Cordon-Cardo, C., Latres, E., Drobnjak, M., Oliva, M. R., Pollack, D., Woodruff, J. M., Marechal, V., Chen, J., Brennan, M. F., and Levine, A. J. Molecular abnormalities of mdm2 and p53 genes in adult soft tissue sarcomas. Cancer Res., *54:* 794–799, 1994.

47. Jones, S. N., Hancock, A. R., Vogel, H., Donehower, L. A., and Bradley, A. Overexpression of Mdm2 in mice reveals a p53-independent role for Mdm2 in tumorigenesis. Proc. Natl. Acad. Sci. USA, *95:* 15608–15612, 1998.

48. Vogelstein, B., and Kinzler, K. W. p53 function and dysfunction. Cell, *70:* 523–526, 1992.

49. Thomas, A., El Rouby, S., Reed, J. C., Krajewski, S., Silber, R., Potmesil, M., and Newcomb, E. W. Drug-induced apoptosis in B-cell chronic lymphocytic leukemia: relationship between p53 gene mutation and bcl-2/bax proteins in drug resistance. Oncogene, *12:* 1055–1062, 1996.

50. Kroemer, G., and Reed, J. C. Mitochondrial control of cell death. Nat. Med., *6:* 513–519, 2000.

51. Reed, J. C. Apoptosis-regulating proteins as targets for drug discovery. Trends Mol. Med., *7:* 314–319, 2001.

52. Budihardjo, I., Oliver, H., Lutter, M., Luo, X., and Wang, X. Biochemical pathways of caspase activation during apoptosis. Annu. Rev. Cell Dev. Biol., *15:* 269–290, 1999.

53. Schwartz, G. K., Farsi, K., Maslak, P., Kelsen, D. P., and Spriggs, D. Potentiation of apoptosis by flavopiridol in mitomycin-C-treated gastric and breast cancer cells. Clin. Cancer Res., *3:* 1467–1472, 1997.

54. Edelman, M. J., Mullins, B., Mack, P. C., Gumerlock, P. H., and Gandara, D. R. Synergistic interaction between flavopiridol (FLAVO) and Taxol (TAX) in a p53-null non-small cell lung carcinoma (NSCLC) cell line. Proc. Am. Assoc. Cancer Res., *39:* 309–310, 1998.

55. Makhija, S., Jusain, A., Schwartz, G. K., and Spriggs, D. R. Cytotoxicity of flavopiridol in ovarian cancer cells, alone and in combination with CDDP. Proc. Am. Assoc. Cancer Res., *38:* 320, 1997.

Molecular Cancer Therapeutics

Flavopiridol Induces Apoptosis in Glioma Cell Lines Independent of Retinoblastoma and p53 Tumor Suppressor Pathway Alterations by a Caspase-independent Pathway[1]

Michelle Alonso, Cristina Tamasdan, Douglas C. Miller, et al.

Mol Cancer Ther 2003;2:139-150.